










The Utility of 18F-FDG PET/CT in Patients With Clinical Suspicion of Polymyalgia Rheumatica and Giant Cell Arteritis: A Prospective, Observational, and Cross-sectional Study

Amir Emamifar,^{1,2,3}  Torkell Ellingsen,^{1,4}  Søren Hess,^{1,5}  Oke Gerke,^{1,4}  Rasmus Hviid Larsen,²
Ziba Ahangarani Farahani,⁴ Per Syrak Hansen,²  Inger Marie Jensen Hansen,²  Henrik Petersen,^{1,4} 
Niels Marcussen,^{1,4}  Michael Dahlstrøm,² Pia Toftegaard,² and Peter Thye-Rønn^{1,2} 

Objective. To define the proportions of agreement between fluorine-18-fluorodeoxyglucose (18F-FDG) positron emission tomography/computed tomography (PET/CT), clinical diagnosis, and temporal artery biopsy (TAB) in patients with polymyalgia rheumatica (PMR) and giant cell arteritis (GCA). Furthermore, the association of 18F-FDG PET/CT uptake patterns and clinical presentation of newly diagnosed PMR and GCA was investigated.

Methods. Eighty patients newly suspected of having PMR, GCA, or concomitant PMR and GCA were included and followed for 40 weeks. Every patient underwent an 18F-FDG PET/CT scan before or within 3 days of initiation of steroids in case of GCA. FDG uptakes in 8 paired articular/periarticular sites and 14 arterial segments were evaluated based on a 4-point visual grading scale.

Results. Of the 80 patients (female: 50 [62.5%]; mean age \pm SD: 72.0 \pm 7.9), 64 (80.0%) patients were diagnosed with pure PMR, 3 (3.7%) with pure GCA, and 10 (12.5%) with concomitant PMR and GCA. Additionally, three (3.7%) patients were diagnosed with seronegative rheumatoid arthritis during the follow-up period. For the diagnosis of PMR, 18F-FDG PET/CT had a proportion of agreement of 75.3 (64.2–84.4), compared with clinical diagnosis. When comparing findings of 18F-FDG PET/CT with TAB, 18F-FDG PET/CT had a proportion of agreement of 93.0 (84.3–97.7) in all included patients and 69.2 (38.6–90.9) in the subgroup of patients with vasculitis. C-reactive protein was significantly higher in patients with PMR activity on 18F-FDG PET/CT compared with those without 18F-FDG PET/CT activity (P value = 0.006).

Conclusions. 18F-FDG PET/CT is a powerful imaging technique in PMR and GCA that was in good agreement with clinical diagnosis and TAB.

INTRODUCTION

Prompt and accurate diagnosis of polymyalgia rheumatica (PMR) and giant cell arteritis (GCA) is critical to initiate corticosteroid treatment and prevent ischemic complications of GCA. In this regard, several imaging modalities, including ultrasound, magnetic resonance imaging, computed tomography

(CT), and fluorine-18-fluorodeoxyglucose positron emission tomography/CT (18F-FDG PET/CT), have been introduced to help confirm the diagnosis. The recent European League Against Rheumatism (EULAR) recommendations for the use of imaging in large-vessel vasculitis in clinical practice emphasizes the need for an early and complementary imaging test, but there is still debate over the most appropriate test (1,2). Recently, 18F-FDG PET/CT

ClinicalTrials.gov Identifier: NCT02985424

The present study is funded by the region of Southern Denmark, the Danish Rheumatism Association, Department of Medicine at Svendborg Hospital, University of Southern Denmark, Odense University Hospital, and A.P Møller Fonden.

¹Amir Emamifar, MD, Torkell Ellingsen, MD, PhD, Søren Hess, MD, Oke Gerke, PhD, Henrik Petersen, MD, Niels Marcussen, MD, Peter Thye-Rønn, MD, PhD: University of Southern Denmark, Odense, Denmark; ²Amir Emamifar, MD, Rasmus Hviid Larsen, MD, Per Syrak Hansen, MD, Inger Marie Jensen Hansen, MD, PhD, Michael Dahlstrøm, MD, Pia Toftegaard: Svendborg Hospital, OUH, Svendborg, Denmark; ³Amir Emamifar, MD: Odense Patient

data Explorative Network (OPEN), Odense, Denmark; ⁴Torkell Ellingsen, MD, PhD, Oke Gerke, PhD, Ziba Ahangarani Farahani, MD, Henrik Petersen, MD, Niels Marcussen, MD: Odense University Hospital, Odense, Denmark; ⁵Søren Hess, MD: Hospital of Southwest Jutland, Esbjerg, Denmark.

No potential conflicts of interest relevant to this article were reported.

Address correspondence to Amir Emamifar, MD, University of Southern Denmark, Department of Clinical Research, Faculty of Health Sciences, Baagøes Allé 15, 5700 Svendborg, Denmark. E-mail: Amir.Emamifar@rsyd.dk.

Submitted for publication May 31, 2020; accepted in revised form June 3, 2020.

has been investigated in a number of PMR and GCA studies, and they've shown high diagnostic accuracy for the detection of both PMR and GCA (3). It can detect extracranial involvement of the large vessels, ie, aorta and its main branches, and is also beneficial to reveal occult malignancy that mimicks the symptoms of PMR and GCA (4–6). GCA may involve the aorta and its major branches, and it characterizes a subset of disease, namely large-vessel GCA (LV-GCA) (7,8). GCA poses several diagnostic challenges. Although with moderate sensitivity, temporal artery biopsy (TAB) is still considered the gold standard for the diagnosis of cranial-GCA (C-GCA) (9,10). However, TAB is invasive and may alter disease management in only a few patients (11). In patients with LV-GCA, classic cranial symptoms are less frequent, and diagnosis of vasculitis often relies on imaging findings (8). Additionally, about 10% to 30% of patients presenting with pure PMR have underlying GCA (12).

Until now, the attenuated diagnostic performance of 18F-FDG PET/CT after initiation of corticosteroids as well as its inability to detect inflammation in the cranial arteries has been considered a downside to 18F-FDG PET/CT. However, the results of a recent Danish study demonstrated the existence of a diagnostic window of opportunity within the 3 days of initiation of high-dose corticosteroids in patients with LV-GCA (13). Moreover, 18F-FDG PET/CT demonstrated high sensitivity and specificity in detecting inflamed cranial arteries in steroid-naïve C-GCA patients, using an elaborate and time-consuming technique, which suggests that TAB could be eliminated (14).

Taking all these considerations into account, in the present study we aimed to explore the association of 18F-FDG PET/CT uptake patterns and the clinical presentation of newly diagnosed PMR and GCA. Furthermore, the proportions of agreement between 18F-FDG PET/CT, TAB, and clinical diagnosis of PMR and GCA were investigated.

MATERIALS AND METHODS

Study design and setting. This is a prospective, observational, and cross-sectional study. The study was performed at the Diagnostic Center, Svendborg Hospital, in collaboration with the section of Rheumatology, Svendborg Hospital, Svendborg, between February 2018 and December 2019. The 18F-FDG PET/CT scans were undertaken at the Department of Nuclear Medicine, Odense University Hospital. Ethical approval was obtained from the Regional Ethics Committee of the Region of Southern Denmark (identification number: S-20160098) and the Danish Data Protection Agency (J.nr 16/40522). This study was also registered at ClinicalTrials.gov (Identifier: NCT02985424).

Participants. Patients who were newly suspected of having PMR, GCA, or concomitant PMR and GCA and who were referred from primary care physicians or hospitalized at our hospital were considered for entry into the study after initial clinical and

paraclinical investigation at the Diagnostic Center. All suspected patients were consecutively screened to see if they met the inclusion criteria that is described in the protocol (15,16). Briefly, to fulfill suspected PMR, five components of the following criteria had to be present: age 50 years or older, bilateral shoulder or hip pain, morning stiffness lasting more than 45 minutes, elevated erythrocyte sedimentation rate (ESR), elevated C-reactive protein (CRP), and disease duration of more than 2 weeks.

Regarding C-GCA, the following criteria were considered: age 50 years or older and elevated ESR/CRP, together with at least two symptoms related to vasculitis (scalp tenderness, vision disturbances, headache (new or changed), jaw claudication, or tenderness of the temporal arteria) (17). However, one cranial symptom was enough to suspect C-GCA in patients also suspected of having concomitant PMR. Patients with clinical suspicion of LV-GCA (ie, upper-extremity claudication and upper-extremity blood pressure discrepancies) were also eligible for inclusion.

Patients were not included in the study if they met one of the following exclusion criteria:

1. Infections, malignancy, or any other conditions where prednisolone was permanently unsuitable.
2. Contraindication to 18F-FDG PET/CT (blood glucose >145 mg/dL after 6 hours fasting)
3. Initiation of steroid treatment more than 3 days prior to 18F-FDG PET/CT.
4. Inability to provide informed consent
5. Patients with dementia or inability to communicate in Danish.

Data collection. Patients' demographics, clinical evaluation, Charlson comorbidity index score (18), laboratory tests, TAB results, and 18F-FDG PET/CT scan findings were collected and managed by means of REDcap (Research Electronic Data Capture), which is a secure, web-based software platform designed to support data capture for research studies at the Open Patient data Explorative Network (19).

Demographic data, clinical evaluation, and Charlson comorbidity index score were recorded at enrollment after provision of informed consent. As a routine procedure in our center, all referred patients were asked to provide blood samples the same day or a day before the initial visit at the Diagnostic Center, which facilitated the process of making the diagnosis and enrolling the patients shortly thereafter.

18F-FDG PET/CT imaging as the index test. Every included patient underwent an 18F-FDG-PET/CT scan before or within 3 days of initiation of steroids in the case of GCA. Results of 18F-FDG PET/CT scan were blinded to both the treating clinicians and patients, and clinical information other than project inclusion was blinded to the nuclear medicine physicians.

18F-FDG PET/CT was performed according to department protocol based on the European Association of Nuclear Medicine

(EANM) guidelines on a GE Discovery PET/CT scanner (General Electric) (20,21). The scan field of view was 70 cm. Attenuation correction was based on the low-dose CT scan. The PET data were reconstructed into transaxial slices with a matrix size of 256×256 (pixel size = 2.74 mm) and a slice thickness of 3.75 mm using iterative 3D ordered subset expectation maximization (3 iterations, 24 subsets) with corrections for time-of-flight (GE VPFx) and point-spread-blurring (GE sharpIR). Corrections for attenuation, randoms, deadtime, and normalization were done inside the iterative loop. Analysis of low-dose CT, PET, and fused PET/CT data was done on a GE Advantage Workstation v. 4.4. Prior to the scan, patients fasted for at least 6 hours and for 60 minutes after injection of a weight-adjusted dose FDG of 4 MBq/kg (minimum: 200 MBq, maximum: 400 MBq). During scanning, patients' arms were positioned above the head. A low-dose CT without contrast enhancement was obtained from the vertex of the skull to the proximal femora for anatomic correlation and attenuation correction of PE images.

Image analysis. 18F-FDG PET/CT images were not initially assessed routinely but only evaluated with regards to incidental findings requiring further diagnostic interventions. Such findings were relayed to the treating clinicians. The full sets of scans were reviewed by two experienced nuclear medicine physicians at the

Department of Nuclear Medicine, who were blinded to all clinical and laboratory data. FDG uptake patterns were recorded in a descriptive manner in 8 paired articular/periarticular sites—ie, shoulder joints (including acromioclavicular joint), sternoclavicular joints, interspinous ligament, hip joints (including iliopsoas bursa), greater trochanter, symphysis pubis enthesis, ischial tuberosity, bursae interspinous (cervical/lumbar)—and 14 arterial segments—ie, aorta, subclavian, axillary, common carotid, internal carotid, external carotid, vertebral, temporal, maxillary, basilar, common iliac, internal iliac, external iliac, and femoral—for each individual patient. FDG uptakes in these sites were evaluated based on a four-point visual grading scale (VGS), as described in earlier studies, with 0 = no uptake, 1 = slight but not negligible uptake, lower than liver uptake, 2 = intermediate uptake, equivalent to liver uptake, 3 = high-grade uptake, higher than liver uptake (22–24). Each site was assessed by both readers individually, and then a consensus FDG uptake grade was determined for each articular/periarticular site as well as arterial segments in every individual patient. We evaluated FDG uptake as being pathologic and nonpathologic with two different VGS cutoffs. Initially, pathologic and nonpathologic uptakes were considered as VGS of 3 or more and less than 3, respectively. At the next step, we reanalyzed our results, whereas VGS of 2 or more and less than 2 were defined as pathologic and nonpathologic uptakes, respectively, because

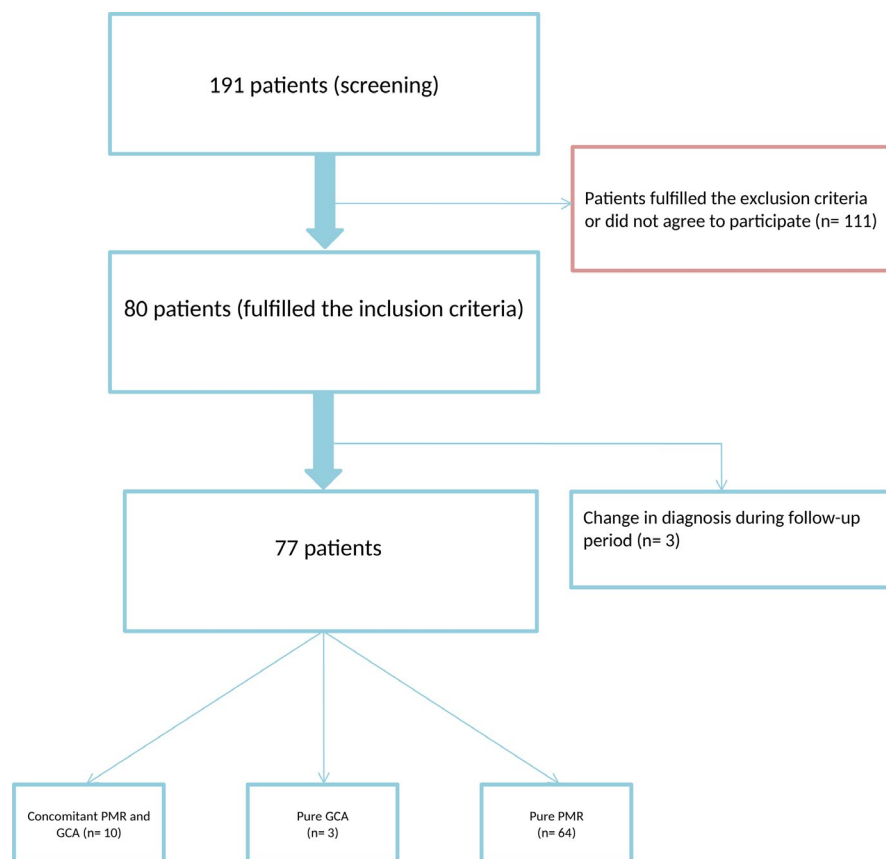


Figure 1. Patient flow diagram. GCA, giant cell arteritis; PMR, polymyalgia rheumatica.

there was no consensus in the available literature. Total PMR and GCA scores were derived from the sum of VGS in each articular/periarticular site and arterial segment, respectively.

The 18F-FDG PET/CT scan was considered positive for PMR if there was a pathologic uptake at any articular/periarticular sites and positive for GCA if there was a pathologic uptake at any arterial segments.

Clinical diagnosis as a reference test. PMR is a clinical diagnosis, and in case of GCA, TAB suffers from a lack of sensitivity as mentioned earlier. Based on the written protocol, all patients were followed for 40 weeks after the initial diagnosis. This time point was sufficient for the clinicians to confirm or reject the diagnosis of PMR and GCA. This method was previously used in several leading studies (10,25). To ensure that clinical diagnosis was made independently from the index test, treating clinicians were blinded with regard to 18F-FDG PET/CT findings during the follow-up, except incidental findings that required further diagnostic workup. We did not change our clinical diagnoses after unrevealing the 18F-FDG PET/CT results because 18F-FDG PET/CT is still under investigation for its future potential in clinical use.

TAB as a gold standard for GCA. All included patients were asked to do a unilateral TAB. The unilateral TAB was taken at the otolaryngology section at our hospital according to the current guideline (26). In patients with cranial symptoms, TAB was taken from the symptomatic side. Results of TAB were described as active arteritis, healed arteritis, suspect for vasculitis, normal or arteriosclerotic, and not representative. Active arteritis on TAB was initially considered a positive result. For further investigation, we reanalyzed our data considering active arteritis and healed arteritis as positive results. The pathologists were blinded to the 18F-FDG PET/CT findings, but not to the clinical data, as these were accessible through patients' medical records.

Not all patients were steroid-naïve at the time of TAB, as previously shown vessel wall infiltrates persisted over months to years after steroid treatment (27). The TAB procedure was described in detail in the protocol (15).

Statistical analysis. Data are presented as means (\pm SD) or (SEM) or median (interquartile range) depending on their distributions. Comparisons of the data between patients with 18F-FDG PET/CT uptakes compatible with pure PMR, pure GCA, concomitant PMR and GCA, and neither PMR nor GCA were made with the Kruskal-Wallis test. A comparison of two binary variables was performed using the Chi-squared test. Total PMR (range: 0-24) and GCA (range: 0-42) scores were defined as the sum of VGS in each articular/periarticular site and arterial segment, respectively. When the score differed from right to left side, the highest score was considered. Wilcoxon rank-sum test (Mann-Whitney *U* test) was used to compare total PMR and GCA scores in patients with and

without PMR and GCA symptoms (ie, constitutional, shoulder and hip girdles, cranial) as well as VGS for each articular/periarticular and arterial segment between two clinical diagnoses. Correlation analysis was performed using Spearman correlation coefficients (r_s). Proportions of agreement (primary analysis) between 18F-FDG PET/CT findings and clinical diagnosis of PMR as well as 18F-FDG PET/CT findings and TAB for the diagnosis of GCA were calculated. Furthermore, sensitivity, specificity, positive predictive value, and negative predictive value were assessed using either clinical diagnosis or TAB as the reference, supplemented by 95% confidence intervals (95% CI). Exploratory data-driven cutoff values were also determined for optimal sensitivity and specificity, in case of PMR. A *P* value was considered significant if *P* < 0.05. No method of imputation was used for missing data. The statistical analysis plan is presented as an appendix. Statistical analysis was performed using STATA version 16.0 (StataCorp). Graphs were plotted using STATA and *ems* package in R program version 3.6.

RESULTS

In total, 191 consecutive patients, referred to the Diagnostic Center with suspected PMR or GCA, were screened to be included in the study. One hundred eleven patients fulfilled the exclusion criteria or did not agree to participate. Eighty patients who fulfilled the inclusion criteria and were willing to give written consent were included in the study. Three patients were diagnosed with seronegative rheumatoid arthritis during 40 weeks of follow-up (Figure 1). The baseline characteristics of patients together with clinical examinations, lab results, and initial prednisolone dose are summarized in Table 1.

Pathology results of TAB. Out of 80 patients, 9 patients did not agree to undergo TAB. Of those from whom biopsy was taken (*n* = 71), four (5.6%) patients had active arteritis and three (4.2%) had healed arteritis on TAB (Supplementary Table 1). The median interval between initial diagnosis and TAB was 7 (interquartile range: 6-10) days. In patients with the clinical diagnoses of pure GCA (*n* = 3) and concomitant PMR and GCA (*n* = 10), TAB showed active arteritis in three (100%) and one (10%) patients, respectively. Three (4.7%) out of 64 patients with pure PMR had signs of healed arteritis on TAB.

18F-FDG PET/CT results. Results of 18F-FDG PET/CT according to clinical diagnoses are summarized in Table 2 and Supplementary Table 2. Increased FDG uptakes in paired articular/periarticular sites in PMR and arterial segments in GCA are illustrated in Figure 2 and Figure 3. Out of 64 patients with the clinical diagnosis of pure PMR, 1 (1.6%) (pathologic uptake cutoff of ≥ 3) and 6 (9.4%) (pathologic uptake cutoff of ≥ 2) patients showed signs of vasculitis on 18F-FDG PET/CT, depending on the cutoff values used for definition of pathologic uptakes. Twenty-one

Table 1. Baseline characteristic of the patients (n = 80)

Baseline characteristic of the patients	Results (n = 80)
Age, y	72.0 ± 7.9
Female gender, n (%)	50 (62.5%)
Body mass index*, kg/m ²	25.4 (22.0-27.9)
Smoking status, n (%)	
Never smoker	27 (33.7%)
Smoker (including former smoker)	53 (66.2%)
Alcohol status, n (%)	
≤6 units per week	58 (72.5%)
>6 units per week	22 (27.5%)
Duration of symptoms before diagnosis, n (%)	
2-4 weeks	18 (22.5%)
5-8 weeks	33 (41.2%)
9-16 weeks	17 (21.2%)
17-24 weeks	5 (6.2%)
>24 weeks	7 (8.7%)
Initial symptoms, n (%)	
Weight loss	31 (38.7%)
• Weight loss*, kg	4 (2-5)
Tiredness	76 (95.0%)
Fever	17 (21.2%)
Neck pain	54 (68.3%)
Shoulder pain	71 (88.7%)
Arm pain	70 (87.5%)
Thigh pain	65 (82.3%)
Buttock pain	65 (81.2%)
Other joints pain	31 (38.7%)
Morning stiffness	66 (83.5%)
• Morning stiffness*, min	60 (30-120)
Arm claudication	26 (32.9%)
Scalp pain	7 (8.7%)
New or changed headache	15 (18.7%)
Jaw claudication	11 (13.7%)
Visual disturbances	15 (18.7%)
Pain in temporal area	10 (12.5%)
Patients pain VAS score*	75 (50-80)
Patients global VAS score*	80 (60-90)
Physician global VAS score*	30 (25-40)
Clinical diagnosis based on initial symptoms, n (%)	
Pure PMR	64 (80.0%)
Pure GCA	3 (3.7%)
Concomitant PMR and GCA	10 (12.5%)
Seronegative RA	3 (3.7%)
Charlson comorbidity index score*	3 (2.5-4)
Physical examination	
Left systolic blood pressure*, mm/Hg	137 (127.5-152)
Right systolic blood pressure*, mm/Hg	135 (124-147)
Left diastolic blood pressure, mm/Hg	82.1 ± 10.7
Right diastolic blood pressure, mm/Hg	80.1 ± 11.4
Left radial pulse, per minute	76.4 ± 13.4
Right radial pulse, per minute	75.6 ± 13.7
Temperature*, °C	36.8 (36.6-37.2)
Neck tenderness to palpitation, n (%)	15 (21.4%)
Shoulder tenderness to palpitation, n (%)	20 (28.6%)
Arm tenderness to palpitation, n (%)	30 (42.9%)
Buttock tenderness to palpitation, n (%)	23 (32.9%)
Thigh tenderness to palpitation, n (%)	27 (38.6%)
Restricted shoulder motion, n (%)	63 (88.7%)
Temporal area tenderness to palpitation, n (%)	5 (7.7%)
Nonpulsatile temporal artery, n (%)	5 (7.1%)

(Continued)

Table 1. (Cont'd)

Baseline characteristic of the patients	Results (n = 80)
Scalp tenderness to palpitation, n (%)	4 (5.7%)
Lab results, [reference values]	
Hemoglobin*, mmol/L [8.3-10.5]	7.6 (7.2-8.2)
Leucocytes*, 10E9/L [3.50-8.80]	9.4 (8.0-11.1)
Platelet*, 10E9/L [145-350]	347.5 (294-446.5)
Albumin*, g/L [34-45]	41 (39-43)
Vitamin D, nmol/L [50-160]	82.2 ± 29.8
ESR*, mm [2-20]	53 (38-77)
CRP*, mg/L [<6.0]	37 (17-63)
Fibrinogen*, μmol/L [5.2-12.6]	15 (13.1-17.2)
Immunoglobulin A*, g/L [0.70-4.30]	2.7 (2.0-3.6)
Immunoglobulin G*, g/L [6.1-15.7]	10.1 (8.7-11.9)
Immunoglobulin M*, g/L [0.40-2.30]	0.8 (0.5-1.3)
Serum-free light chains*, [0.60-1.56]	1.2 (1.0-1.5)
RF positive, n (%)	8 (10%)
Anti-CCP positive, n (%)	3 (3.7%)
ANA positive, n (%)	16 (20.2%)
C-ANCA positive, n (%)	2 (2.6%)
P-ANCA positive, n (%)	1 (1.3%)
Prednisolone initial dose, mg/d*	20 (20-40)

Note. Results are presented as numbers (percentage), mean ± SD, or *median (interquartile range) depending on their distribution.

Abbreviations: ANA, antinuclear antibody; anti-CCP: anti-cyclic citrullinated peptide; C-ANCA, cytoplasmic-antineutrophil cytoplasmic antibody; CRP, C-reactive protein; ESR, erythrocyte sedimentation rate; GCA, giant cell arteritis; P-ANCA, perinuclear-antineutrophil cytoplasmic antibody; PMR, polymyalgia rheumatica; RA, rheumatoid arthritis; RF, rheumatoid factor; VAS, visual analogue scale.

patients with a pathologic uptake cutoff value of 3 or more (26.2%) and seven patients with a pathologic uptake cutoff value of 2 or more (8.7%) did not show pathologic FDG uptakes in any articular/periarticular sites or arterial segments.

The mean ± SEM for total PMR and GCA scores were 12.2 ± 0.7 and 0.8 ± 0.2, respectively. The mean (SEM) of VGS for each articular/periarticular site as well as arterial segment in patients whose diagnoses of PMR, GCA, or concomitant PMR and GCA were confirmed during follow-up (n = 77) are illustrated in Figures 4A and 4B. Ischial tuberosity, hip joint (including iliopsoas bursa), shoulder joint (including acromioclavicular joint), and greater trochanter had the highest FDG uptakes (Figure 4A). In the case of GCA, the highest FDG uptakes were detected in subclavian, axillary, vertebral, and basilar arteries consecutively (Figure 4B). No FDG uptakes in temporal and maxillary arteries were found. The mean ± SEM of VGS for each articular/periarticular site as well as arterial segment in patients with clinically confirmed diagnoses of PMR, GCA, or concomitant PMR and GCA are presented in Table 3.

VGS values for ischial tuberosity, hip joint (including iliopsoas bursa), shoulder joint (including the acromioclavicular joint), and greater trochanter were significantly higher in patients with pure PMR than in those with pure GCA and concomitant PMR and GCA. VGS for subclavian, basilar, vertebral, and femoral arteries were statistically significantly higher in patients with pure GCA than

Table 2. Results of 18F-FDG PET/CT based on clinical diagnosis (pathologic cutoff of ≥ 3)

18F-FDG PET/CT results	Pure PMR n = 64	Pure GCA n = 3	PMR + GCA n = 10	Seronegative RA n = 3	Total n = 80
PMR activity	51 (79.7%)	0 (0%)	4 (40%)	1 (33.3%)	56 (70.0%)
GCA activity	0 (0%)	1 (33.3%)	1 (10%)	0 (0%)	2 (2.5%)
PMR and GCA activity	1 (1.6%)	0 (0%)	0 (0%)	0 (0%)	1 (1.2%)
Neither PMR nor GCA activity	12 (18.7%)	2 (66.7%)	5 (50%)	2 (66.7%)	21 (26.2%)

Abbreviations: 18F-FDG, fluorine-18-fluorodeoxyglucose; CT, computed tomography; GCA, giant cell arteritis; PET, positron emission tomography; PMR, polymyalgia rheumatica; RA, rheumatoid arthritis.

in patients with pure PMR. Additionally, VGS values for aorta, subclavian, axillary, common carotid, basilar, and vertebral arteries were higher in patients with concomitant PMR and GCA compared with patients with pure PMR, and the results were statically significant.

None of the articular/periarticular sites and arterial segments showed a statistically significant difference of VGS in patients with pure GCA compared with patients with concomitant PMR and GCA when there was FDG uptake in at least one patient.

Agreement between 18F-FDG PET/CT, TAB, and clinical diagnosis. For the diagnosis of PMR, 18F-FDG PET/CT had a proportion of agreement of 75.3 (64.2-84.4) (Table 4 and Supplementary Table 3).

Considering the total PMR score, a cutoff value of 9 (out of 24) had the highest level of accuracy at 81.5% with a proportion of agreement of 80, sensitivity of 79.7%, specificity of 83.3%, positive predictive value of 98.3%, and negative predictive value of 25%. Further increase in the cutoff value increased

specificity, though sensitivity decreased dramatically (Supplementary Figure 1).

The proportion of agreement for the diagnosis of GCA, with 18F-FDG PET/CT and TAB, in the included patients is summarized in Table 5 and Supplementary Table 4. When comparing findings of 18F-FDG PET/CT to TAB, 18F-FDG PET/CT had a proportion of agreement of 93.0 (84.3-97.7) when considering positive TAB as active arteritis (Table 5). Considering positive TAB as active and healed arteritis, 18F-FDG PET/CT had a proportion of agreement of 88.7 (79.0-95.0) (Supplementary Table 5).

In a subgroup analysis in those with vasculitis, ie, patients with pure GCA and concomitant PMR and GCA, 18F-FDG PET/CT had a proportion of agreement of 69.2 (38.6-90.9) when compared with TAB (Table 6 and Supplementary Table 6). When considering positive TAB as active arteritis and healed arteritis, the results did not change because no healed arteritis was found in these subgroups of patients as earlier reported in Supplementary Table 1.

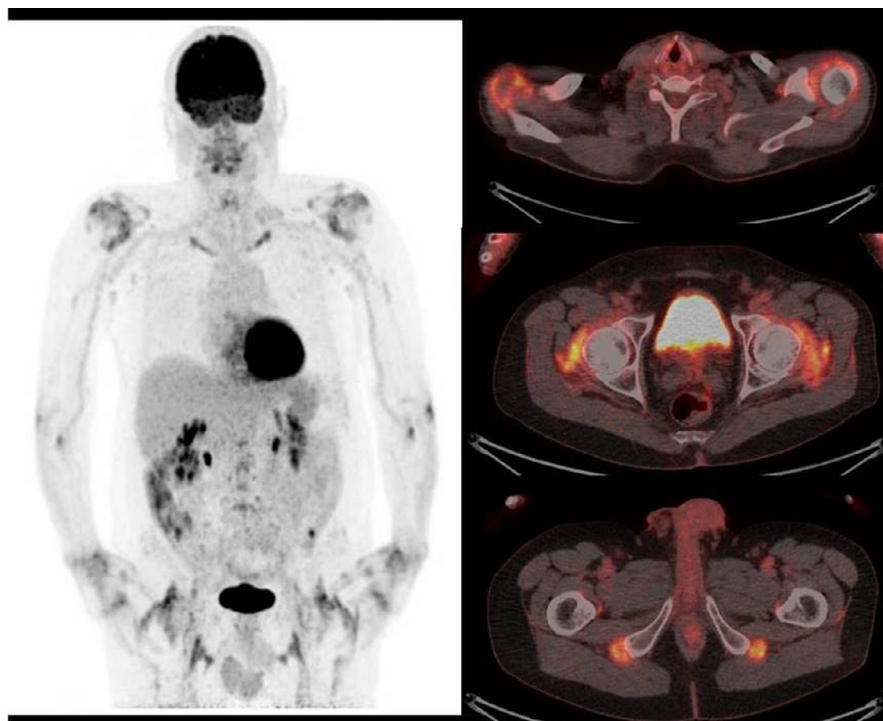


Figure 2. FDG-PET whole-body MIP image (left column) and fused axial FDG-PET/CT images shows increased FDG uptake in the soft tissues around the shoulders and hips and bilaterally at the ischial tuberosity. FDG uptake is clearly higher than liver uptake, ie, level 3 uptake, and thus categorized as pathologic.

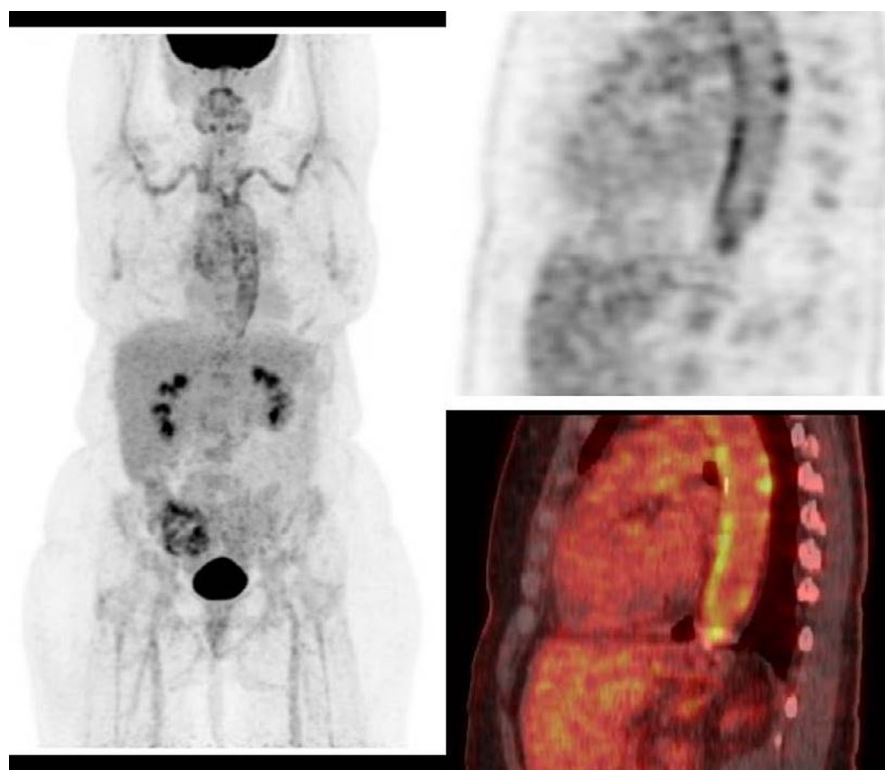


Figure 3. FDG-PET whole-body MIP image (left) and sagittal PET (upper right) and fused PET/CT (lower right) images of the aorta shows increased FDG uptake in the thoracic aorta, subclavian arteries and axillary arteries. FDG-uptake is clearly higher than liver uptake, ie, level 3 uptake, and thus categorized as pathologic. Note nodular calcification in the aorta without FDG uptake. This finding together with the diffuse FDG uptake along the vascular wall also points to vasculitis rather than atherosclerosis as the underlying etiology for FDG uptake.

Association between clinical data and total VGS for PMR and GCA in patients with clinically confirmed diagnoses of PMR, GCA, or concomitant PMR and GCA. A summary of exploratory correlations between clinical data and total VGS for PMR and GCA can be found in Supplementary Table 7.

There was a significant moderate correlation between total VGS for PMR and CRP ($r_s = 0.35$, $P = 0.005$). Additionally, total VGS for PMR and GCA showed a significant, weak, and negative correlation ($r_s = -0.29$, $P = 0.025$). Supplementary Figure 2 illustrates the differences for total VGS for PMR and GCA between each clinical diagnosis, namely pure PMR, pure GCA, and concomitant PMR and GCA. There was a significant difference between total VGS for PMR and GCA when comparing them in patients with pure PMR and pure GCA as well as pure PMR and concomitant PMR and GCA. We found no statistically significant difference neither for total VGS for PMR nor for GCA when comparing them in patients with pure GCA and concomitant PMR and GCA.

Fibrinogen showed a significant correlation to serum levels of CRP ($r_s = 0.60$, $P < 0.0005$) and ESR ($r_s = 0.57$, $P < 0.0005$).

When comparing total PMR and GCA scores in patients with and without constitutional symptoms (weight loss, tiredness, fever), shoulder girdle symptoms (pain and stiffness in neck, shoulder, and upper arm), hip girdle symptoms (pain and stiffness in

buttock and thigh), and cranial symptoms (new or changed headache, jaw claudication, temporal area pain, scalp pain), total PMR score was significantly higher in patients who had shoulder girdle symptoms ($P = 0.040$) and hip ($P = 0.007$) and lower in patients who had cranial symptoms ($P = 0.0001$). In addition, we found a significantly higher total GCA score in patients who had cranial symptoms ($P = 0.0001$) and a lower GCA score in patients who had hip girdle symptoms ($P = 0.011$). No statistically significant differences were found in total PMR and GCA scores in patients with and without constitutional symptoms (Supplementary Table 8).

Correlation analyses between VGS for each articular/periarticular sites as well as arterial segments in patients with clinically confirmed diagnoses of PMR, GCA or concomitant PMR and GCA. Correlations between each articular/periarticular sites as well as arterial segments are presented in Supplementary Tables 9 and 10, respectively. In general, there were several significant correlations between VGS of articular sites in the shoulder and hip girdles (Supplementary Table 9). Besides, in terms of vasculitis, VGS of arterial branches showed significant correlations with their origins—for instance, axillary with subclavian ($r_s = 0.84$, $P < 0.0005$) as well as vertebral with subclavian ($r_s = 0.40$, $P = 0.0003$) arteries (Supplementary Table 10).

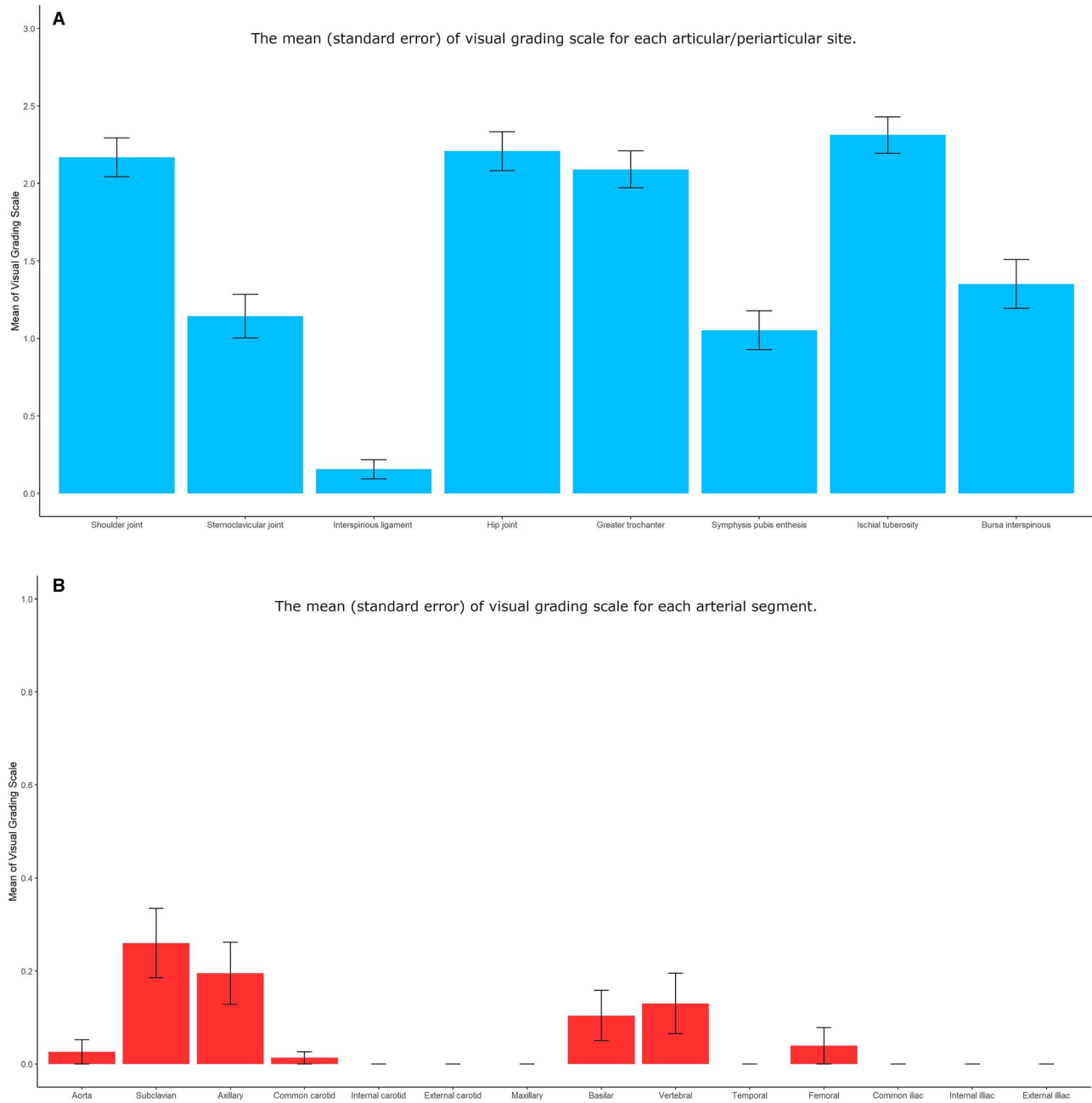


Figure 4. The mean (standard error) of visual grading scale for each articular/periarticular site (A) and arterial segment (B).

Demographical and clinical differences based on 18F-FDG PET/CT findings in patients with clinically confirmed diagnoses of PMR, GCA, or concomitant PMR and GCA. When comparing demographical and clinical data in patients with pathologic 18F-FDG PET/CT uptake of ≥ 3 , compatible with PMR activity, GCA activity, PMR and GCA activity, and neither PMR nor GCA activity, CRP was significantly higher in patients with PMR activity on 18F-FDG PET/CT compared with those without 18F-FDG PET/CT activity (neither PMR nor GCA) ($P = 0.006$). We did not observe any statistical differences

between these groups when a pathologic cutoff value of 2 or more was considered (Supplementary Table 11).

DISCUSSION

The current study prospectively investigated the diagnostic performance of 18F-FDG PET/CT in 80 patients with initial presentation of PMR, GCA, or both compared with the clinical diagnosis of PMR as well as TAB in the case of GCA. For the diagnosis of PMR, 18F-FDG PET/CT had a proportion of agreement of 75.3

Table 3. Visual grading scale for each articular/periarticular site as well as arterial segment according to the clinical diagnoses

	Pure PMR	Pure GCA	Concomitant PMR and GCA	Pure PMR vs Pure GCA <i>P</i> Value ^a	Pure GCA vs Concomitant PMR and GCA <i>P</i> Value ^a	Pure PMR vs Concomitant PMR and GCA <i>P</i> Value ^a
Articular/periarticular sites (mean ± SEM)						
Shoulder joint	2.4 ± 0.1	0.3 ± 0.3	1.4 ± 0.4	0.005	0.18	0.014
Sternoclavicular joint	1.2 ± 0.2	0.3 ± 0.3	0.8 ± 0.3	0.26	0.51	0.38
Interspinous ligament	0.2 ± 0.1	0.0 ± 0.0	0.2 ± 0.2	0.58	0.58	0.93
Hip joint	2.4 ± 0.1	0.3 ± 0.3	1.2 ± 0.4	0.003	0.21	<0.001
Greater trochanter	2.3 ± 0.1	0.3 ± 0.3	1.5 ± 0.3	0.007	0.10	0.021
Symphysis pubis enthesis	1.1 ± 0.1	0.3 ± 0.3	1 ± 0.3	0.27	0.32	0.87
Ischial tuberosity	2.5 ± 0.1	0.3 ± 0.3	1.8 ± 0.4	0.002	0.08	0.052
Bursa interspinous	1.4 ± 0.2	0.7 ± 0.7	1.1 ± 0.5	0.31	0.63	0.52
Arterial segments (mean ± SEM)						
Aorta	0.0 ± 0.0	0.0 ± 0.0	0.2 ± 0.2	...	0.58	0.011
Subclavian	0.1 ± 0.1	1.7 ± 0.9	0.6 ± 0.3	0.001	0.19	0.009
Axillary	0.1 ± 0.0	1.0 ± 1.0	0.6 ± 0.3	0.06	0.85	0.001
Common carotid	0.0 ± 0.0	0.0 ± 0.0	0.1 ± 0.1	...	0.58	0.011
Internal carotid	0.0 ± 0.0	0.0 ± 0.0	0.0 ± 0.0
External carotid	0.0 ± 0.0	0.0 ± 0.0	0.0 ± 0.0
Maxillary	0.0 ± 0.0	0.0 ± 0.0	0.0 ± 0.0
Basilar	0.0 ± 0.0	0.7 ± 0.7	0.3 ± 0.2	0.002	0.57	0.007
Vertebral	0.0 ± 0.0	1.0 ± 1.0	0.5 ± 0.3	0.001	0.57	0.006
Temporal	0.0 ± 0.0	0.0 ± 0.0	0.0 ± 0.0
Femoral	0.0 ± 0.0	1.0 ± 1.0	0.0 ± 0.0	<0.001	0.07	1.0
Common iliac	0.0 ± 0.0	0.0 ± 0.0	0.0 ± 0.0
Internal iliac	0.0 ± 0.0	0.0 ± 0.0	0.0 ± 0.0
External iliac	0.0 ± 0.0	0.0 ± 0.0	0.0 ± 0.0

Bolded values indicate significant results.

Abbreviations: GCA, giant cell arteritis; PMR, polymyalgia rheumatica.

^a *P* values are calculated by Wilcoxon rank-sum test.

(64.2-84.4). Considering the total PMR score, a cutoff value of 9 (out of 24) had the highest level of accuracy of 81.5% with a proportion of agreement of 80, sensitivity of 79.7%, specificity of 83.3%, positive predictive value of 98.3%, and negative predictive value of 25%. Of 64 patients with pure PMR, 1 (1.6%; pathologic uptake cutoff of ≥ 3) and 6 (9.4%; pathologic uptake cutoff of ≥ 2) patients showed signs of vasculitis on 18F-FDG PET/CT. Ischial tuberosity, hip joint (including iliopsopectinal bursae), shoulder joint (including acromioclavicular joint), and greater trochanter had the highest FDG uptakes, and VGS scores for these sites were

Table 4. Agreement between 18F-FDG PET/CT and clinical diagnosis of PMR (pathologic cutoff of ≥ 3)

18F-FDG PET/CT	Clinical Diagnosis –	Clinical Diagnosis +
18F-FDG PET/CT without PMR activity	2	18
18F-FDG PET/CT with PMR activity	1	56
Total assessed	3	74
Proportion of agreement (95% CI)	75.3 (64.2-84.4)	
Sensitivity (95% CI)	75.7% (64.3%-84.9%)	
Specificity (95% CI)	66.7% (9.4%-99.2%)	
Positive predictive value (95% CI)	98.2% (90.6%-100.0%)	
Negative predictive value (95% CI)	10.0% (1.2%-31.7%)	

Abbreviations: 18F-FDG, fluorine-18-fluorodeoxyglucose; CI, confidence interval; CT, computed tomography; PET, positron emission tomography; PMR, polymyalgia rheumatica.

statistically significant and higher in patients with pure PMR than in those with pure GCA and concomitant PMR and GCA patients.

When comparing findings of 18F-FDG PET/CT with TAB, 18F-FDG PET/CT had a proportion of agreement of 93.0 (84.3-97.7) in all included patients and of 69.2 (38.6-90.9) in the subgroup of patients with vasculitis. The highest FDG uptake was detected in subclavian, axillary, vertebral, and basilar arteries, consecutively. No FDG uptakes in temporal and maxillary arteries were reported. Of patients with a cutoff value of 3 or more, or those with a cutoff value of 2 or more, 21 (26.2%) and 7 (8.7%) patients, respectively, did not show pathologic FDG uptakes in any articular/periarticular sites or arterial segments.

A number of previous studies investigated the diagnostic performance of 18F-FDG PET or 18F-FDG PET/CT in patients with PMR, C-GCA, or LV-GCA (5,6,25,28-37). A prospective study by Henckaerts et al determined that in patients with steroid-naïve PMR, a total skeletal score of 16 or more in 12 articular regions (scored on a three-point scoring system with 0 = no FDG uptake; 1 = moderate FDG uptake, less than liver uptake; and 2 = intense FDG uptake, equal or more than liver uptake) had a sensitivity, specificity, positive predictive value, and negative predictive value of 85.1%, 87.5%, 93.4%, and 73.7%, respectively. Signs of vasculitis were observed in 15% of PMR patients in this study (29). Another study by Sondag and colleagues noted that in patients

Table 5. Agreement between 18F-FDG PET/CT and TAB in the included patients, considering TAB positive as active arteritis (pathologic cutoff of ≥ 3)

18F-FDG PET/CT	TAB -	TAB +
18F-FDG PET/CT without GCA activity	65	3
18F-FDG PET/CT with GCA activity	2	1
Total assessed	67	4
Proportion of agreement (95% CI)	93.0 (84.3-97.7)	
Sensitivity (95% CI)	25% (0.6%-80.6%)	
Specificity (95% CI)	97.0% (89.6%-99.6%)	
Positive predictive value (95% CI)	33.3% (0.8%-90.6%)	
Negative predictive value (95% CI)	95.6% (87.6%-99.1%)	

Abbreviations: 18F-FDG, fluorine-18-fluorodeoxyglucose; CI, confidence interval; CT, computed tomography; GCA, giant cell arteritis; PET, positron emission tomography; TAB, temporal artery biopsy.

with newly diagnosed PMR or relapse of PMR compared with patients with neoplasm as a control group, presence of 3 or more sites with significant uptake (cutoff value of ≥ 2 , scored on four-point scale with 0 = no uptake, 1 = slight uptake, 2 = moderate uptake and 3 = uptake higher than the liver) out of 17 different sites had a sensitivity of 74% and specificity of 79%. In this regard, shoulder, ischial tuberosity, interspinous bursae, greater trochanter, and hips had the highest FDG uptake (28). A sensitivity of 79% for diagnosing PMR with the aid of 18F-FDG PET/CT was reported by Lund-Petersen et al in a retrospective study if FDG uptake at any two of the shoulder, hip, and spinous processes were detected. Vascular FDG uptake was seen in 7% of patients, whereas 14% of patients had no uptake or other pathological uptakes (31).

In terms of GCA, estimation of sensitivity and specificity were more complicated because the disease has several subtypes. Though sensitivity and specificity of 18F-FDG PET/CT are mostly described in patients with LV-GCA, which indicates high sensitivity and specificity for diagnosing LV-GCA (30,34,36,37), a few recent studies revealed the high diagnostic performance of 18F-FDG PET/CT in detecting inflammation in the cranial vessels (14,25). For instance in a study by Sammel et al (25) on 64 patients with newly

Table 6. Agreement between 18F-FDG PET/CT and TAB in patients with vasculitis, ie, pure GCA and concomitant PMR and GCA (pathologic cutoff of ≥ 3)

18F-FDG PET/CT	TAB -	TAB +
18F-FDG PET/CT without GCA activity	8	3
18F-FDG PET/CT with GCA activity	1	1
Total assessed	9	4
Proportion of agreement (95% CI)	69.2 (38.6-90.9)	
Sensitivity (95% CI)	25.0% (0.6%-80.6%)	
Specificity (95% CI)	88.9% (51.7%-99.7%)	
Positive predictive value (95% CI)	50.0% (1.3%-98.7%)	
Negative predictive value (95% CI)	72.7% (39.0%-94.0%)	

Abbreviations: 18F-FDG, fluorine-18-fluorodeoxyglucose; CI, confidence interval; CT, computed tomography; GCA, giant cell arteritis; PET, positron emission tomography; PMR, polymyalgia rheumatica; TAB, temporal artery biopsy.

suspected GCA, the sensitivity and specificity of 18F-FDG PET/CT for the diagnosis of GCA were 92% and 85% compared with TAB and were 71% and 91% compared with clinical diagnosis. In their study, the subjective global assessment of the scans was considered as being positive or negative for GCA. This was of great importance when considering the global assessment of the PET/CT scans; as in this study, FDG uptakes were not detected in temporal arteries in approximately 60% of biopsy-positive patients with GCA. Therefore, it can be postulated, for instance if the study population mostly consists of pure C-GCA with individual involvement of the temporal artery, that the sensitivity of 18F-FDG PET/CT will dramatically decline. This was nearly seen in the study by Nielsen et al, in which sensitivity dropped from 82% to 36%, considering FDG uptakes in temporal and/or maxillary and/or vertebral arteries versus only FDG uptakes in temporal artery (14). However, in the Nielsen et al study, PET images were cropped by the investigators to minimize the risk of bias to only include head and neck, and, as a matter of fact, was different in study design from the study by Sammel et al. Compared with the results of our study, 18F-FDG PET/CT did not show high sensitivity for diagnosing GCA when compared with TAB, though it had excellent specificity. This discrepancy was due to the fact that no FDG uptakes in temporal and maxillary arteries were detected in the current study. On the other hand, our study population consisted of both PMR and GCA patients. When we limited our analysis to those with vasculitis, ie, pure GCA and concomitant PMR and GCA, sensitivity was increased to 75% at its best. Furthermore, arm positions (over head or by the side) during scanning might have impacted the 18F-FDG PET/CT results. Nevertheless, the clinical value of 18F-FDG PET/CT might differ in different clinical settings. Though high sensitivity is especially important in malignant diseases in order to not overlook the disease, in rheumatic diseases, specificity could be of more importance in order to not overtreat the patients. This was why we primarily analyzed our data based on the pathologic cutoff value of 3 or more.

One hundred ninety-one patients were referred, often by general practitioners, to our Diagnostic Center and screened for possible inclusion in this study. With the exception of a few patients who did not agree to participate, we found that a considerable number of referred patients with a suspicion of PMR and/or GCA were classified with other diagnoses, mostly musculoskeletal diseases with normal or slightly increased acute phase reactants. This points out the complexity of PMR and GCA diagnoses that still needs more work, though there has been great improvement in recent years.

When comparing demographical and clinical data in patients with 18F-FDG PET/CT uptakes (pathologic cutoff of ≥ 3) compatible with PMR activity, GCA activity, PMR and GCA activity, and neither PMR nor GCA activity, CRP was significantly higher in patients with PMR activity on 18F-FDG PET/CT compared with those without 18F-FDG PET/CT activity (neither PMR nor GCA). However, no statistical differences between these groups were found when a pathologic cutoff value of 2 or more was taken into consideration. Previously, Blockmans et al and Lund-Petersen et al found

no correlation between clinical features and PET findings (5,31). In contrast, Rosenblum et al demonstrated significant associations between clinical factors, ie, age, body mass index, as well as CRP and arterial FDG uptake (38). Additionally, the total PMR score was consistent with patients' symptoms of shoulder and hip, and the total GCA score was consistent with cranial symptoms.

Total VGS for PMR and CRP were moderately correlated ($r_s = 0.35$). Additionally, total VGS for PMR and GCA showed a significant, weak, and negative correlation ($r_s = -0.29$). The latest finding suggests that the higher global burden of PMR on 18F-FDG PET/CT is associated with the lower global burden of vascular involvement. This may indicate that, in clinical practice, the PMR patients presenting with a typical PMR picture, with intensive involvement of shoulder and hip, have a lower risk of vascular involvement compared with those with atypical and milder symptoms. However, because of the exploratory nature of these findings, this should be confirmed by future studies.

The strengths of the current study include the following: Firstly, all PMR patients were steroid-naïve at the time of performing 18F-FDG PET/CT. In the case of GCA, all scans were performed within 3 days of treatment initiation. Secondly, the diagnosis of PMR and GCA was confirmed by 40 weeks of follow-up, which minimized the risk of bias due to misdiagnosis and misclassification. This approach was also described in numbers of previous studies. For instance, in the 2016 TABUL ultrasound study, 6-month follow-up assessment was used to confirm the final diagnosis (10). Thirdly, in all patients—including PMR patients—TAB was performed. Fourthly, nuclear medicine physicians were blinded to the clinical and laboratory data, and treating clinicians were blinded to the findings of 18F-FDG PET/CT during the follow-up period, except for serious incidental findings. Lastly, and more importantly, this study reflected the real-life diagnostic dilemma of PMR and GCA in daily clinical practice and represented a variety of phenotypes of the disease spectrum.

Our study had some limitations. First of all, the imaging interpretation we used in this study was based on visual scoring. This method of interpretation, though commonly used previously, is remarkably investigator dependent with interobserver variability. Furthermore, individual differences in general FDG uptake, distribution, metabolic activity, and the time lapse between injection and scanning may impact uptake in the liver that was the basis for VGS assessment, although steps were taken to standardize the imaging protocol (6). Secondly, 18F-FDG PET/CT was performed within 3 days of treatment initiation in the case of GCA, which was due to fear of ischemic complications and blindness. Although, this exact diagnostic window for performing 18F-FDG PET/CT in new-onset LV-GCA patients has been proposed by Nielsen et al, whether this could be generalized to newly diagnosed C-GCA patients, still needs to be confirmed in future studies (13). Thirdly, cranial vessel uptake assessment in this study was limited to temporal, maxillary, basilar, vertebral, and carotid arteries. However, the involvement of other cranial arteries, for example occipital or

facial, has been addressed in previous studies (25,39). Perhaps, visualization of additional cranial arteries would result in increased sensitivity. At last, our results should be interpreted cautiously in case of GCA, as the number of patients with GCA in our study was limited. It is also worth mentioning that the expected FDG uptake in healed arteritis on TAB is likely less than active arteritis, which is why we analyzed our data on two occasions.

The results of the present study have a high degree of generalizability. Our study population represented a real-life PMR and GCA population with varied phenotypes of the disease and was not limited to a specific subtype of the disease. Furthermore, the VGS used for interpretation of 18F-FDG PET/CT has been frequently used in daily clinical settings. Though 18F-FDG PET/CT is largely accessible in Denmark and expenses are covered by the Danish health insurance system, availability and cost of 18F-FDG PET/CT may hamper the generalizability of this method in some international centers.

To summarize, there is great heterogeneity in the literature regarding the diagnostic performance of 18F-FDG PET/CT in patients with PMR and GCA. This is partly due to the nature of PMR and GCA disease with variable phenotypes and study populations and partly because several methods of assessment are used for interpretation of 18F-FDG PET/CT—ie, the number of sites evaluated, VGS versus semiquantitative assessment (eg, standardized uptake value metric, target-to-background ratios, etc), or both. In conclusion, we found 18F-FDG PET/CT to be a valuable imaging technique in PMR that was in good agreement with clinical diagnosis. Additionally, we found it can detect underlying GCA in patients with PMR. 18F-FDG PET/CT can also help with the diagnostic workup of PMR and GCA patients to rule out other mimics of the disease, especially in the case of PMR. However, particular attention should be paid to the patients with individual inflammation in the cranial arteries, in which the sensitivity of 18F-FDG PET/CT is influenced by the small diameter of these vessels, though with excellent specificity.

ACKNOWLEDGMENTS

The authors would like to thank Mrs. Merete Birkholm Hansen for her contribution to the study coordination. We would also like to thank Mrs. Afsaneh Mohammadnejad for her contribution to data analysis and Mrs. Maryam Mousavi for her contribution to data management. Finally, we would like to thank senior consultants Søren Andreas Just, Anders Jørgen Svendsen, Wolfgang Böhme, and Dr. Susan Due Kay for their professional input.

AUTHOR CONTRIBUTIONS

All authors contributed substantially to drafting the article or revising it critically for important intellectual content. All authors gave final approval of the version of the article to be published.

Study conception and design. Emamifar, Ellingsen, Hess, Jensen Hansen, Thye-Rønn.

Acquisition of data. Emamifar, Ellingsen, Hess, Hviid Larsen, Ahangarani Farahani, Syrak Hansen, Jensen Hansen, Toftegaard, Thye-Rønn.

Analysis and interpretation of data. Emamifar, Ellingsen, Hess, Gerke, Ahangarani Farahani, Syrak Hansen, Jensen Hansen, Petersen, Marcussen, Dahlstrøm, Toftegaard, Thye-Rønn.

REFERENCES

- Dejaco C, Ramiro S, Duftner C, Besson FL, Bley TA, Blockmans D, et al. EULAR recommendations for the use of imaging in large-vessel vasculitis in clinical practice. *Ann Rheum Dis* 2018;77:636–43.
- Hellmich B, Agueda A, Monti S, Buttgerit F, de Boysson H, Brouwer E, et al. 2018 Update of the EULAR recommendations for the management of large vessel vasculitis. *Ann Rheum Dis* 2020;79:19–30.
- Slart RH; Writing group; Reviewer group; Members of EANM Cardiovascular; Members of EANM Infection & Inflammation; Members of Committees, SNMMI Cardiovascular; Members of Council, PET Interest Group; Members of ASNC; EANM Committee Coordinator. FDG-PET/CT(A) imaging in large vessel vasculitis and polymyalgia rheumatica: joint procedural recommendation of the EANM, SNMMI, and the PET Interest Group (PIG), and endorsed by the ASNC. *Eur J Nucl Med Mol Imaging* 2018;45:1250–69.
- Rehak Z, Sprlakova-Pukova A, Kazda T, Fojtik Z, Vargova L, Nemeč P. (18)F-FDG PET/CT in polymyalgia rheumatica—a pictorial review. *Br J Radiol* 2017;90:20170198.
- Blockmans D, Stroobants S, Maes A, Mortelmans L. Positron emission tomography in giant cell arteritis and polymyalgia rheumatica: evidence for inflammation of the aortic arch. *Am J Med* 2000;108:246–9.
- Prieto-González S, Depetris M, García-Martínez A, Espigol-Frigolé G, Tavera-Bahillo I, Corbera-Bellata M, et al. Positron emission tomography assessment of large vessel inflammation in patients with newly diagnosed, biopsy-proven giant cell arteritis: a prospective, case-control study. *Ann Rheum Dis* 2014;73:1388–92.
- Salvarani C, Cantini F, Boiardi L, Hunder GG. Polymyalgia Rheumatica and Giant-Cell Arteritis. *New England Journal of Medicine*. 2002;347:261–271. <https://doi.org/10.1056/nejmra011913>
- Muratore F, Kermani TA, Crowson CS, Green AB, Salvarani C, Matteson EL, et al. Large-vessel giant cell arteritis: a cohort study. *Rheumatology (Oxford)* 2015;54:463–70.
- Ashton-Key MR, Gallagher PJ. False-negative temporal artery biopsy. *Am J Surg Pathol* 1992;16:634–5.
- Luqmani R, Lee E, Singh S, Gillett M, Schmidt WA, Bradburn M, et al. The Role of Ultrasound Compared to Biopsy of Temporal Arteries in the Diagnosis and Treatment of Giant Cell Arteritis (TABUL): a diagnostic accuracy and cost-effectiveness study. *Health Technol Assess* 2016;20:1–238.
- Bowling K, Rait J, Atkinson J, Srinivas G. Temporal artery biopsy in the diagnosis of giant cell arteritis: does the end justify the means? [cohort study]. *Ann Med Surg (Lond)* 2017;20:1–5.
- González-Gay MA, Matteson EL, Castañeda S. Polymyalgia rheumatica. *Lancet* 2017;390:1700–12.
- Nielsen BD, Gormsen LC, Hansen IT, Keller KK, Therkildsen P, Hauge EM. Three days of high-dose glucocorticoid treatment attenuates large-vessel 18F-FDG uptake in large-vessel giant cell arteritis but with a limited impact on diagnostic accuracy. *Eur J Nucl Med Mol Imaging* 2018;45:1119–28.
- Nielsen BD, Hansen IT, Kramer S, Haraldsen A, Hjorthaug K, Bogsrud TV, et al. Simple dichotomous assessment of cranial artery inflammation by conventional 18F-FDG PET/CT shows high accuracy for the diagnosis of giant cell arteritis: a case-control study. *Eur J Nucl Med Mol Imaging* 2019;46:184–93.
- Emamifar A, Hess S, Gerke O, Hermann AP, Lastrup H, Hansen PS, et al. Polymyalgia rheumatica and giant cell arteritis—three challenges—consequences of the vasculitis process, osteoporosis, and malignancy: a prospective cohort study protocol. *Medicine (Baltimore)* 2017;96:e7297.
- Dasgupta B, Salvarani C, Schirmer M, Crowson CS, Maradit-Kremers H, Hutchings A, et al. and members of the American College of Rheumatology Work Group for Development of Classification Criteria for PMR. Developing classification criteria for polymyalgia rheumatica: comparison of views from an expert panel and wider survey. *J Rheumatol* 2008;35:270–7.
- Hunder GG, Bloch DA, Michel BA, Stevens MB, Arend WP, Calabrese LH, et al. The American College of Rheumatology 1990 criteria for the classification of giant cell arteritis. *Arthritis Rheum* 1990;33:1122–8.
- Charlson ME, Pompei P, Ales KL, MacKenzie CR. A new method of classifying prognostic comorbidity in longitudinal studies: development and validation. *J Chronic Dis* 1987;40:373–83.
- Open Patient data Explorative Network. URL: https://open.rsyd.dk/index_en.html.
- Jamar F, Buscombe J, Chiti A, Christian PE, Delbeke D, Donohoe KJ, et al. EANM/SNMMI guideline for 18F-FDG use in inflammation and infection. *J Nucl Med* 2013;54:647–58.
- Boellaard R, Delgado-Bolton R, Oyen WJ, Giammarile F, Tatsch K, Eschner W, et al. and the European Association of Nuclear Medicine (EANM). FDG PET/CT: EANM procedure guidelines for tumour imaging: version 2.0. *Eur J Nucl Med Mol Imaging* 2015;42:328–54.
- Meller J, Strutz F, Siefker U, Scheel A, Sahlmann CO, Lehmann K, et al. Early diagnosis and follow-up of aortitis with [(18)F]FDG PET and MRI. *Eur J Nucl Med Mol Imaging* 2003;30:730–6.
- Goerres GW, Forster A, Uebelhart D, Seifert B, Treyer V, Michel B, et al. F-18 FDG whole-body PET for the assessment of disease activity in patients with rheumatoid arthritis. *Clin Nucl Med* 2006;31:386–90.
- Walter MA, Melzer RA, Schindler C, Müller-Brand J, Tyndall A, Nitzsche EU. The value of [18F]FDG-PET in the diagnosis of large-vessel vasculitis and the assessment of activity and extent of disease. *Eur J Nucl Med Mol Imaging* 2005;32:674–81.
- Sammel AM, Hsiao E, Schembri G, Nguyen K, Brewer J, Schrieber L, et al. Diagnostic accuracy of positron emission tomography/computed tomography of the head, neck, and chest for giant cell arteritis: a prospective, double-blind, cross-sectional study. *Arthritis Rheumatol* 2019;71:1319–28.
- Foghsgaard LJ. Arteria temporalis-biopsi. *Ugeskr Læger* 2006;168:1774–5.
- Maleszewski JJ, Younge BR, Fritzlen JT, Hunder GG, Goronzy JJ, Warrington KJ, et al. Clinical and pathological evolution of giant cell arteritis: a prospective study of follow-up temporal artery biopsies in 40 treated patients. *Mod Pathol* 2017;30:788–96.
- Sondag M, Guillot X, Verhoeven F, Blagosklonov O, Prati C, Boulahdour H, et al. Utility of 18F-fluoro-dexoxyglucose positron emission tomography for the diagnosis of polymyalgia rheumatica: a controlled study. *Rheumatology*. 2016;55: 1452–1457. <https://doi.org/10.1093/rheumatology/kew202>
- Henckaerts L, Gheysens O, Vanderschueren S, Goffin K, Blockmans D. Use of 18F-fluorodeoxyglucose positron emission tomography in the diagnosis of polymyalgia rheumatica—A prospective study of 99 patients. *Rheumatology*. 2018;57:1908–1916. <https://doi.org/10.1093/rheumatology/kex376>
- Grayson PC, Alehashemi S, Bagheri AA, Civelek AC, Cupps TR, Kaplan MJ, et al. 18 F-Fluorodeoxyglucose-Positron Emission Tomography As an Imaging Biomarker in a Prospective, Longitudinal Cohort of Patients With Large Vessel Vasculitis. *Arthritis Rheumatol* 2018;70:439–449. <https://doi.org/10.1002/art.40379>
- Lund-Petersen A, Voss A, Lastrup H. PET-CT findings in patients with polymyalgia rheumatica without symptoms of cranial ischaemia. *Dan Med J* 2017;6464:pji: A5410.

32. Yamashita H, Kubota K, Takahashi Y, Minaminoto R, Morooka M, Ito K, et al. Whole-body fluorodeoxyglucose positron emission tomography/computed tomography in patients with active polymyalgia rheumatica: evidence for distinctive bursitis and large-vessel vasculitis. *Mod Rheumatol* 2012;22:705–11.
33. Blockmans D, De Ceuninck L, Vanderschueren S, Knockaert D, Mortelmans L, Bobbaers H. Repetitive 18-fluorodeoxyglucose positron emission tomography in isolated polymyalgia rheumatica: a prospective study in 35 patients. *Rheumatology (Oxford)* 2007;46:672–7.
34. Lee YH, Choi SJ, Ji JD, Song GG. Diagnostic accuracy of 18F-FDG PET or PET/CT for large vessel vasculitis: a meta-analysis. *Z Rheumatol* 2016;75:924–31.
35. Besson FL, Parienti JJ, Bienvenu B, Prior JO, Costo S, Bouvard G, et al. Diagnostic performance of ¹⁸F-fluorodeoxyglucose positron emission tomography in giant cell arteritis: a systematic review and meta-analysis. *Eur J Nucl Med Mol Imaging* 2011;38:1764–72.
36. Fuchs M, Briel M, Daikeler T, Walker UA, Rasch H, Berg S, et al. The impact of 18F-FDG PET on the management of patients with suspected large vessel vasculitis. *Eur J Nucl Med Mol Imaging* 2012;39:344–53.
37. Soussan M, Nicolas P, Schramm C, Katsahian S, Pop G, Fain O, et al. Management of large-vessel vasculitis with FDG-PET: a systematic literature review and meta-analysis. *Medicine (Baltimore)* 2015;94:e622.
38. Rosenblum JS, Quinn KA, Rimland CA, Mehta NN, Ahlman MA, Grayson PC. Clinical factors associated with time-specific distribution of 18F-fluorodeoxyglucose in large-vessel vasculitis. *Sci Rep* 2019;9:15180.
39. Ješe R, Rotar Ž, Tomšič M, Hočevar A. The role of colour Doppler ultrasonography of facial and occipital arteries in patients with giant cell arteritis: a prospective study. *Eur J Radiol* 2017;95: 9–12.